

# Squeezapulse: Adding Interactive Input to Fabricated Objects Using Corrugated Tubes and Air Pulses

Liang He\*

Gierad Laput†

Eric Brockmeyer†

Jon E. Froehlich\*

\* University of Maryland, College Park, Maryland, United States

† Carnegie Mellon University, Pittsburgh, Pennsylvania, United States

\* {lianghe, jonf}@cs.umd.edu, † gierad.laput@cs.cmu.edu, † ebrockme@andrew.cmu.edu



Figure 1. We introduce *Squeezapulse*, a technique for creating interactive fabricated objects using acoustic sensing without external circuitry or power but one single microphone. Above, four example applications show the flexibility and value of our approach: (a) a gamepad controller; (b) a soft and interactive bunny; (c) a squeezable phone case; and (d) a force sensor.

## ABSTRACT

We present *Squeezapulse*, a technique for embedding interactivity into fabricated objects using soft, passive, low-cost bellow-like structures. When a soft cavity is squeezed, air pulses travel along a flexible pipe and into a uniquely designed corrugated tube that shapes the airflow into predictable sound signatures. A microphone captures and identifies these air pulses enabling interactivity. We describe the underlying acoustic theory used to inform our design, an informal examination of the effect of different 3D-printed corrugations on air signatures, and our resulting *Squeezapulse* implementation. To demonstrate and evaluate the potential of *Squeezapulse*, we present four prototype applications and a small, lab-based user study ( $N=9$ ). Our evaluations show that our approach is accurate across users and robust to external noise. We conclude with a discussion of limitations and future work.

## Author Keywords

Fabricated objects; passive acoustic sensing; soft cavity; pipe; squeeze interactions; corrugated tube; air pulse.

## ACM Classification Keywords

H.5.2. Information interfaces and presentation (e.g., HCI): Input devices and strategies.

Permission to make digital or hard copies of all or part of this work for personal or classroom use is granted without fee provided that copies are not made or distributed for profit or commercial advantage and that copies bear this notice and the full citation on the first page. Copyrights for components of this work owned by others than ACM must be honored. Abstracting with credit is permitted. To copy otherwise, or republish, to post on servers or to redistribute to lists, requires prior specific permission and/or a fee. Request permissions from Permissions@acm.org. TEI '17, March 20-23, 2017, Yokohama, Japan

© 2017 ACM. ISBN 978-1-4503-4676-4/17/03...\$15.00  
DOI: <http://dx.doi.org/10.1145/3024969.3024976>

## INTRODUCTION

Fabrication techniques such as 3D printing, laser cutting, and casting have been increasingly used to build physical prototypes in HCI. Incorporating interactive functions into fabricated objects, however, is still a cumbersome and highly decoupled process. In response, an emerging body of work aims to imbue fabricated objects with interactive capabilities throughout the rapid prototyping cycle, including via custom-designed optics [36], touch sensitive electronics [29], active acoustic-enabled structures [11], and precision sensors [35]. Building on this growing literature, we introduce *Squeezapulse*, a technique for creating interactive fabricated objects using acoustic sensing without embedded circuitry, wiring, or power (Figure 1). Our novel approach shapes small puffs of air into identifiable but inaudible sound signatures via custom fabricated structures.

We were inspired by passive airflow mechanisms in bellows and accordions, which were designed to furnish strong blasts of air without requiring external power. We synthesize similar principles for constructing simple *squeezable units* that can be used for input control. *Squeezapulse* is comprised of three core parts: (i) a soft and squeezable cavity to generate airflow; (ii) a tube designed with specific inner-wall corrugations to shape the airflow into unique acoustic signatures, effectively acting as a physical filter [2]; and (iii) a microphone connected to a computer that classifies these signatures for interactive inputs. Figure 2 provides an illustrative example of creating an interactive 3D-printed bunny. Because each tube produces a unique signature, only a single embedded microphone is necessary to sense multiple inputs. To verify

the feasibility and the accuracy of our approach, we built four prototype applications and present results from a lab-based study with nine participants.

In summary, our work contributes: (i) a passive acoustic sensing and machine learning-based approach for recognizing distinct puffs of air; (ii) a distillation of design implications for fabricating corrugated tubes for robust and accurate sensing; (iii) and a wide range of illustrative applications across different prototyping platforms, demonstrating feasibility and accuracy. Since our approach relies on the detection of passive puffs of air, we are not limited to “squeeze” interactions. Any technique that generates air puffs (*e.g.*, blowing) offers an additional avenue for making fabricated objects interactive. We discuss these and other application areas in the Discussion.

## RELATED WORK

Our work builds on prior research in the areas of prototyping interactive objects, acoustic sensing, and squeezable interfaces.

*Prototyping and Fabrication of Interactive Objects.* Making things interactive is an essential part of physical prototyping in HCI. As noted in the Introduction, a large body of emerging work has begun to explore how to embed interactivity into the ever-growing repertoire of fabricated objects (*e.g.*, 3D prints). For example, 3D-printed, optically clear pipes have been used for sensing, displaying, and embedding interactive elements [1,36]. Broader approaches have also been explored, including linear arrays of strain gauges[13], computer vision techniques [26] and generic tubular pathways [28], all of which offer the potential to transform plastic or photopolymer-based 3D prints into interactive objects. Beyond rigid outputs, additive manufacturing-based fabrication of soft materials have also been investigated, including techniques for embedding tightly-coupled electronics into layers of felt or fabric [8,23]. Although these efforts require designers to embed particular structures in the model (*e.g.*, optically clear tubes or print voids), they nonetheless offer the unique ability to reduce the need for traditional electronic circuitry. Likewise, our approach offers similar tradeoffs. Further, our approach aims at providing a robust and reusable mechanism (*i.e.*, corrugated tubes) that could be attached on different fabricated objects for interactive controls.

*Acoustic Sensing as Input.* A large body of work in HCI has explored acoustic-based sensing across multiple interactive applications. Approaches can be categorized as active [5,11,16,19], which recognize user input by relying on a sustained source of sound such as from a sweep frequency generator, or passive [6,7,8,10,18,22,24,27], which do not require electronically generated sounds. Our work builds on the growing area of using passive acoustics for interaction—in particular, interactive acoustic sensing with custom-designed, 3D-printed structures. For example, *Tickers* [31] is a labeling toolkit that uses printed percussion instruments to label different 3D-printed objects. *Acoustic*

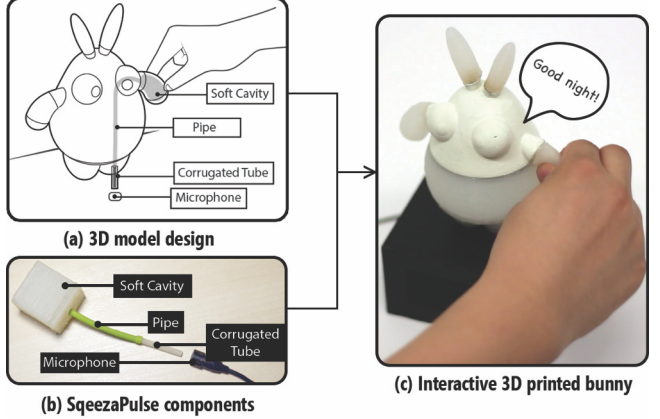


**Figure 2.** Squeezapulse uses soft cavities, flexible pipes, and corrugated tubes to enable interactive fabricated objects. Shown above, a user squeezes a soft hand embedded into a 3D-printed bunny, which generates an identifiable air pulse. While we depict only one input above, the interactive bunny actually has six squeezable cavities—each cavity is connected to its own uniquely designed corrugated tube which leads to a single shared microphone, which is the basis of our approach. See the supplementary video for a demo.

*Voxels* [12] builds a wide range of acoustic filter applications by embedding a matrix of primitives inside 3D-printed objects. Additionally, *Cilllia* [20] senses acoustic input based on printed fur on the arbitrary surface of 3D-printed objects. Closest to our work is *Lamello* [27], an acoustic model-based approach using comb-like structures for real-time processing of computational events. While Lamello enables new interactive input on 3D-printed objects, the approach is limited to strikes generated by the movement of physical components as input. Together, the above techniques highlight the breadth, scalability, and practicality of passive acoustic sensing techniques.

*Soft Interfaces for Squeeze Interactions.* Prior work has investigated squeeze interactions with soft primitives or objects, which can enable new, playful and innovative interfaces [3,4]. For instance, *Skweezee* [34] explored design implications for squeeze interactions based on hand gesture training and testing on large squeezable primitives. In practice, integrating deformable structures and material could add rich interactions to daily objects. For example, *Squeeze Me* [14] mounts a squeezable cover on a tablet providing expressive human robot interactions. *FuwaFuwa* [10] is a sensor module that can be embedded and used for measuring the deformation of soft objects such as cushions and plush toys. Likewise, soft sensors, which are made of soft and elastic material (*e.g.*, silicone, flexible 3D printing filament), could also support interactive controls by using pneumatics [15,18,32,37], or using special-purpose pressure sensors, as in the work by *Slyper* and colleagues [33]. Our approach allows designers to prototype squeezable interactions with the deformable and soft parts embedded in general fabricated objects.

In summary, our work introduces a novel passive sensing approach for prototyping interactive objects, solely relying on pulses of air, without additional sensors, circuitry, or complex mechanisms, except for a single microphone. Previous approaches require either an active source of sound (*e.g.*, [11] uses speakers and ultrasound) or individual sensor pairs (*e.g.*, in [32], each block requires individual pressure sensors). Unlike prior work, our approach does not require an active sound or pressure source, which is cumbersome and noisy. Further, our corrugated tubes are easy to fabricate and are reusable.

### THEORY OF OPERATION

Our approach is based on corrugated acoustic theory [2]. Air flow through corrugated pipes can be manipulated and shaped by different corrugation designs [24]. To dampen or alter sound in airflow systems, corrugated pipes are found in a range of industrial and domestic applications such as air conditioning systems, vacuum cleaners, musical toys (*e.g.*, [24]), and flexible risers in the oil industry.

Corrugated acoustic theory is based on two fundamental concepts: *standing waves* and the *Cummings acoustic model* [24]. Standing waves are common in wind and brass instruments which are tube shaped (*e.g.*, flute). The sound frequency, amplitude, harmonics, and timbre of the standing wave are affected by the properties of the tube. Interestingly, whether the tube is straight or bent (*e.g.*, into circles) has minimal impact on the generated sound, although a very sharp bend does have some effect [30]. Thus, we use flexible tubes as channels for transmitting air flow from the soft cavity to corrugated tubes.

Based on the principles of standing waves, the Cummings acoustic model [24] is widely used to inform the design of large corrugated pipes. In this model, air flow, and therefore the resulting sound, is shaped by the velocity of sound  $c_0$ , the tube's length  $L$ , tube's inner radius  $R$ , the volume of the cavity between two consecutive corrugations, the area presented by the cavity to the tube, and the spatial period of corrugations (pitch)  $P_c$ . More precisely, the diagram of corrugated tube is illustrated in Figure 3, where  $d$  is the height of the corrugation. The relationship between these factors is shown in (1), where wave number  $n = 1, 2, 3\dots$ , representing a group of generated frequencies.

In our work, we parameterized and explored the corrugated tubes based on the aforementioned theories (Figure 3). While these theories may be directly codified into a rule-based classifier, in our preliminary experiments we found that a machine learning-based empirical approach performed better, perhaps accounting for small deformities in tube design due to fabrication limitations.

### DESIGN SPACE OF CORRUGATED TUBES

As noted above, corrugated tube length, gaps between corrugations, corrugation shapes, and corrugation distributions play key roles in characteristically altering airflow. While exhaustively exploring each permutation and

combination is intractable, we opted instead to select 12 corrugated tubes that contained exemplar parameters (through trial and error). Once selected, we then conducted one-to-one comparisons to help us fully understand how these form factors characteristically alter transient puffs of air. This work extends the explorations conducted in *Acousturments* [11], with a particular novel focus on investigating the interior texture of the tubes and its impact on spectral signatures.

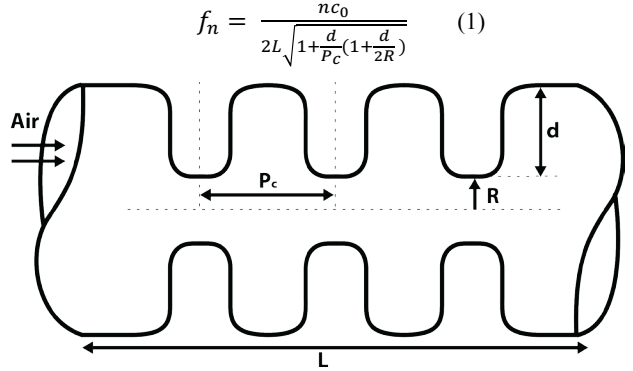
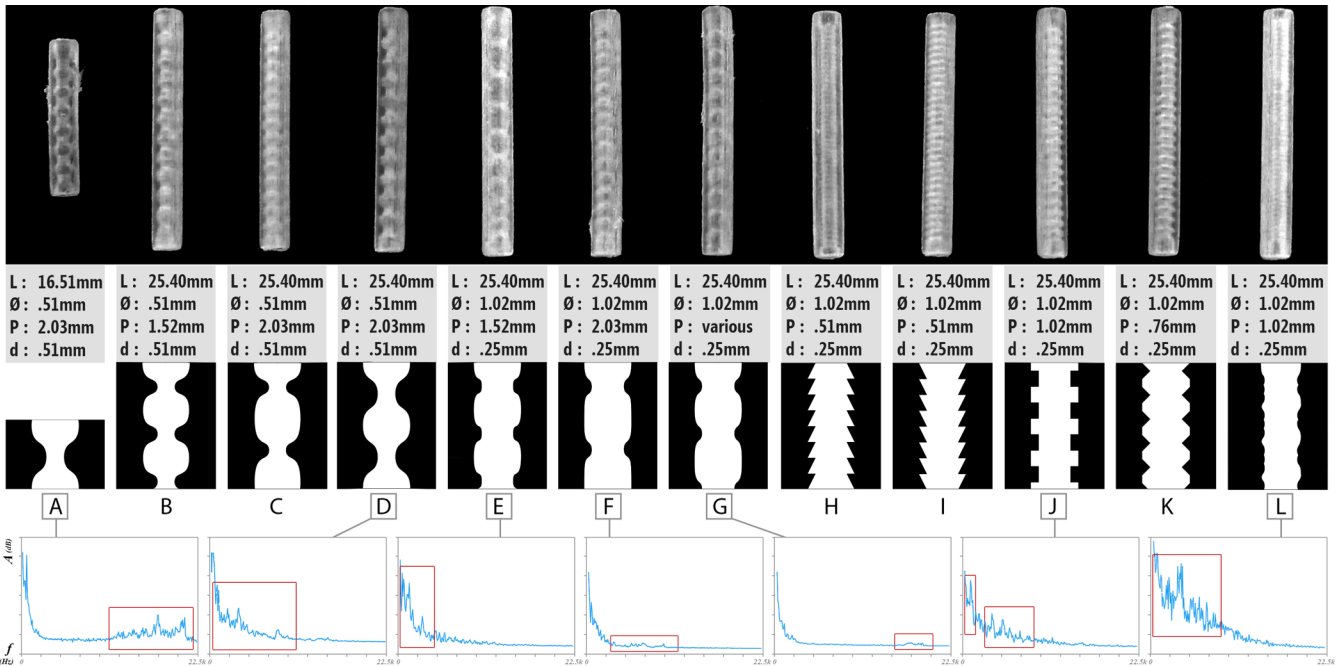


Figure 3. A corrugated tube diagram and equation.

Before we began our design space explorations, we tested the “strength” of the air pulse on 3D-printed pipes with different interior diameters. In general, thin pipes are better at preserving air energy and diameters between 1.6-3.2 mm produced superior performance. Bigger diameters resulted in weaker pulses while thinner ones blocked air flow. Additionally, as expected [24], we found that the outputted signal is proportional to the strength of the input air puff and that it attenuates as the tube becomes longer. In our trials, most air pulses were detectable using tubes that were 25 cm or shorter. We observed that air puffs passing through corrugated tubes had a significant effect on uniquely shaping acoustic signatures (qualitatively verified through visual inspection of the spectrogram). Because we rely on air pulses, our technique makes slightly audible but faint sound bursts.

To investigate how tube design directly affects the eventual output signal, we used the model in corrugated acoustics for guidance and performed side-by-side comparisons of two representative tubes that differed in one controlled parameter (*e.g.*, tube length). As shown in Figure 4, we experimented with: different lengths (*e.g.*, Tube A vs. Tube D), inner tube diameters (*e.g.*, Tube D vs. Tube F), the distance between two consecutive corrugations (*e.g.*, Tube E vs. Tube F), corrugate shapes (*e.g.*, Tube E vs. Tube J), and corrugation distributions (*e.g.*, only Tube L has an asymmetric corrugation distribution). We studied discrete parameters of corrugated tubes for the purpose of exploring how physical factors affect the production of air puffs, since there is a lack of evidence in theory showing if it works with small fabricated parts having imprecise corrugations (*e.g.*, 3D-printed tubes). In the next section, we describe the results of these informal experiments.



**Figure 4.** We conducted an informal exploration of corrugation variables that affect airflow, including: L: length,  $\emptyset$ : inner diameter, P: distance between corrugations, d: corrugation height. (Top row) actual 3D-printed tubes. (Middle row) corresponding diagrammatic views with parameters. (Bottom row) magnitude spectrums of signal generated through the representative corrugated tubes. The red rectangles in the plots highlight characteristically different energies across spectral signatures.

### Corrugated Tube Length

To experiment with the effect of tube length on sound, we designed two tubes with similar corrugations but different lengths (Tube A and Tube D). As Figure 4 shows, air flow through a longer corrugated tube produces sound with energy at lower frequency bands, which is aligned with the Cummings model. As the length decreases, the energy of the spectrum shifts toward higher bands.

### Corrugated Tube Inner Diameter

We also altered the tube's inner diameter. Again, our experiments confirmed theoretical predictions. The signal generated by a smaller diameter has more power at higher frequency bands while the output caused by a bigger diameter has more power at lower bands (*i.e.*, a smaller diameter tube produces higher pitch sounds). As Tube D and Tube F demonstrate, a mere 0.5mm disparity is sufficient to produce characteristic changes in the spectral signal.

### Corrugation Distribution

The overall distribution of corrugations within a tube's interior wall also influences airflow, although it is not predictable by the learned model. With a symmetrical distribution, the output spectrum (Tube E) looks smoother than that out of an asymmetrical distribution (Tube L). Nonetheless, both variations show energy levels centered around lower frequency bands.

### Space between Corrugations

The distance between successive corrugations can also impact airflow. In Figure 4, the group of Tube E and Tube F shows that only a small increase in interval distance

between two corrugations can result in dramatic changes in air pulse generation. In the output of Tube F, the spectrum looks more flat than that of Tube E. In addition to uniformly distributed corrugations, incremental gaps also lead to slight differences in frequency output. As seen in Tube G, increasing gaps between corrugations generates tiny peaks among higher frequency bands and is sufficient for characteristically altering the spectral signal, which can eventually be used for input detection.

### Corrugation Shape

Internally, corrugations can have uniquely varying shapes (*e.g.*, cubic, sawtooth ridges, sinusoidal contours, *etc.*). The corrugation surface can alter the reflection path of the passing sound waves, which results in the variation of frequency in the output. Tube E and Tube J illustrates a comparison of curved and cubic corrugations. Although the profiles of both output frequencies are similar, cubic corrugation causes more peaks among the middle frequency bands, which is highly differentiable.

### Exploring Simultaneous Inputs

While not a physical property of the corrugated tubes themselves, we also wanted to explore whether our approach could be used to detect *simultaneous* inputs using a *single* microphone. From our experiments, we observed that the spectral results produced by individual air structures can be simply “summed up,” forming a new combined output that is distinct enough to be identified by the microphone. Similar to single inputs, all combinations of simultaneous inputs require training for recognition. Additionally, we observed that our approach could support

the detection of multiple types of squeezing on a single soft cavity (as long as the squeeze creates an observable signal, see Bunny and deformable pressure sensor examples).

## IMPLEMENTATION

Squeezapulse is comprised of three core parts: (i) a soft and squeezable *cavity*, (ii) a *corrugated tube* and (iii) a *microphone*. The cavity and the corrugated tube are hidden inside the body of an object and connected to a flexible latex pipe. When a soft cavity is squished, it produces a blast of air that tunnels through the corrugated tube, characteristically altering the sound wave, and then through the latex pipe to an awaiting microphone. Using supervised learning, we can identify these unique pulses of air and use them to build interactive fabricated objects.

To build a Squeezapulse object, one must first convert a portion of their fabricated design into a soft and squeezable cavity, then connect a 3D-printed corrugated tube using a latex pipe, and finally position an electret condenser microphone next to the outlet of the corrugated tube. Multiple soft cavities and corrugated tubes can exist in the fabricated object if unique corrugations are used for each embedded tube. Below, we describe the fabrication of the soft cavities and corrugated tubes as well as our passive sensing approach.

## Fabrication

Our soft cavities are made of silicone rubber compounds, but other approaches are likely possible (e.g., elastic printing filament such as TangoPlus<sup>1</sup>). To simplify our process, we 3D-printed molds for silicone casting (analogous to that in [37]) with a regular desktop 3D printer (e.g., MakerBot) and PLA or ABS filament. Further, we used Sil-Poxy glue to bond silicone with other plastic 3D-printed parts. We found that silicone casting works well at a low cost. For example, for a 2.6 cc model, it only costs ~\$0.20, a win compared to traditional methods for 3D printing soft cavities (e.g., \$4.50 via Objet Connex, which is a constant print cost). For precision purposes, we printed our corrugated tubes from bottom to top along with the axes of the tube in an Objet Eden260V printer with a resolution of 600 dpi (42 microns) and clear UV-cured photopolymer. Theoretically, 3D printers with a resolution of at least 0.2mm should work.

## Passive Acoustic Sensing

We use an off-the-shelf microphone for capturing air pulses (*Audio-technica ATR3350*). The incoming audio data is recorded as a linear Pulse-Code Modulation (PCM) (sampling rate: 44kHz), and stored in a circular buffer (buffer size:  $5 \times 1024$ ). Before any further processing, we compute the Root Mean Square (RMS) of the captured audio to detect steady state (inactive) vs. squeezed state (active). If the onset is met, the data in the buffer is transformed into frequency domain using a Fast Fourier

Transformation (FFT). Next, we downsample the raw FFT data into 128 bins and use it to derive more features: band ratios, mean, standard deviation, min index, max index, center of mass, and spectral kurtosis. These features are fed into a machine learning algorithm, where we utilize a Support Vector Machine model (SVM) for either classification or regression (the latter is used for estimating squeeze strength). For classification, we trained a Sequential Minimal Optimization (SMO)-based SVM using default optimization parameters (kernel=polynomial, C=100, e=1.0). For regression, we optimized a SMOreg using the polykernal with default optimization parameters. Both models are provided by the library of Weka<sup>2</sup>, and they work for all computation executed on a *MacBook Pro (Core 2 Duo, SD-Mid 2009)* with a ~50ms latency.

## EXAMPLE APPLICATIONS

To demonstrate the viability of our approach, how it integrates with existing fabrication techniques (e.g., 3D printing), and to touch on different points in our design space, we prototyped four example Squeezapulse applications. To view working demonstrations, see the supplementary video uploaded with the paper.

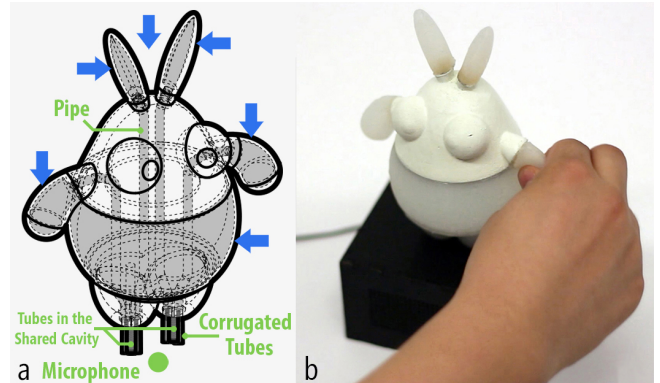


**Figure 5.** The interactive bunny: (a) interact with the bunny by squeezing soft parts (gray areas); (b) squeezing the bunny in real world. Blue arrows point to squeezable, interactive areas.

*Interactive Toy.* We created an interactive 3D-printed bunny doll with soft ears, hands, and body built on a base box, which encloses the microphone (Figure 5). We replaced both ears, hands, and the belly with soft cavities (gray areas in Figure 5). All soft parts are connected to the bottom microphone through pipes inside the bunny's body. Six different corrugated tubes (two were attached to the large cavity of the belly) were used with one shared microphone to distinguish inputs. Besides pressing each cavity, our prototype also supports simultaneous squeeze inputs, (e.g., multiple combinations of squeezing both ears and hands). Interestingly, poking and pressing the belly could be differentiated by our approach, because they cause different deformations on the soft belly and therefore affect the air flows through two different corrugated tubes (the two

<sup>1</sup> <http://www.stratasys.com/materials/polyjet/rubber-like>

<sup>2</sup> <http://www.cs.waikato.ac.nz/ml/weka/>

corrugated tubes in the belly cavity). These inputs were programmed to support interactive storytelling, such as playing a character-driven sound or animation.

*Deformable Force Sensor.* To demonstrate how our approach can estimate squeeze strength, we made a simple force sensor using a regression-based model. In this example, squeezing is performed on a large soft pad, embedded within in a rigid 3D-printed case (Figure 6a). When the pad is pressed, the ratio between the estimated force and the maximum pressure value is shown on screen (Figure 6b). We trained a regression-based model using data samples collected at three equally spaced pressure levels (no pressure, half pressure, and full pressure).



Figure 6. The force sensor: (a) pressing the soft pad generates an air flow; (b) detecting different pressure force.

*Gamepad.* Instead of a game controller with rigid buttons, we built a gamepad controller with five soft buttons (Figure 7), which provides a more natural feeling. Four cubic pads serve as directional buttons that receive touch-up and touch-down events, while a circular button (center) offers a selection-type input (*e.g.*, a click event). All buttons were embedded in a clear case fabricated using laser-cut acrylic pieces, bonded layer by layer. Together, this prototype offers a multi-input passive device for controlling games. For example, in a Pac-man game, the user can control the character’s movements by pressing the four directional buttons, while the central button can be used to change the character’s properties (*e.g.*, body color).

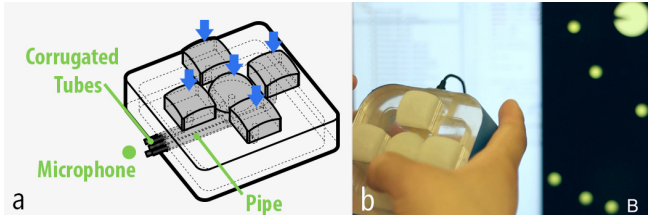


Figure 7. The gamepad: (a) pressing each soft button on the game controller generates a puff of air; (b) playing a Pac-Man game using our gamepad.

*Smart Case.* We also built a 3D-printed case for a handheld device with two soft buttons on the side to encourage eyes-free, tangible interaction while also limiting screen occlusion (Figure 8). These buttons can be used to power interactive applications on the phone. For example, for controlling a music player without waking up the screen, for snoozing or turning off an alarm clock without looking at the phone screen, and for capturing a photo with one hand when the other hand is occupied.

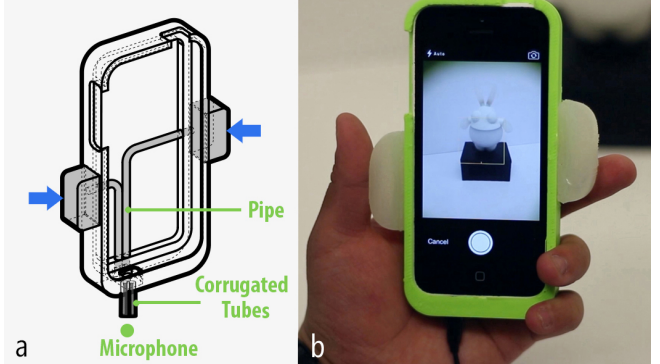


Figure 8. The smart case: (a) squeezing soft buttons generates air flows; (b) squeezing both buttons to take a photo.

## EVALUATION

Our evaluations sought to answer the following questions: (i) How accurately can we classify unique air puffs? (ii) How robust are our classifiers when trained per-user *vs.* cross-user? (iii) How robust is our approach to noise? To address these questions, we conducted a user study with nine participants (aged 23–29, five female). We focused on evaluating our three classification-based applications: the gamepad, the interactive bunny, and the smart case. We also describe a follow-up noise robustness experiment.

## Procedure

The study was conducted in our lab and included a 30-minute data collection session. Before the start of each session, an experimenter briefed participants and showed them how to use the prototypes. Participants were encouraged to interact with the prototypes in whichever way they wanted during data collection to improve ecological validity. All participants followed the same sequence of directed interactions starting with the gamepad controller, the bunny, and then the smart case. Participants performed specific interactions after hearing a beep sound. We collected two rounds of data for each prototype and recorded 30 samples of each interaction per round. We also collected 60 samples per prototype of ‘noisy’ data. For this, participants were asked to make noise on and around the device by tapping, repositioning, knocking, talking, *etc.* but to not actually press a soft button or cavity. These samples were used to evaluate *false positives* and *true negatives*.

In total, we collected 12,420 interactions—1,380 per participant (see Table 1). For the gamepad controller, we recorded press-down and press-up events on each directional button (four buttons; eight events total) and a click event on the central button. For the interactive bunny, we recorded individual cavity squeezes (four total), simultaneous squeeze inputs (both ears and both hands; two events total) and multiple inputs on one single cavity (press down on head to compress belly and poke belly; two events total). For the smart case, individual and simultaneous squeezing on soft buttons were trained (two buttons; three events total).

Prototype	Soft Button/Cavity	Interaction	# of Samples/Person
Gamepad	Left, right, top, down buttons	Press down	60 of each (240 total)
	Left, right, top, down buttons	Press up	60 of each (240 total)
	Center button	Click	60
	N/A	Noise	60
Bunny	Left & right ear; left & right hand	Squeeze	60 of each (240 total)
	Both ears, both hands	Simultaneous squeeze	60 of each (120 total)
	Body press	Press down	60
	Body poke	Poke	60
Smart Case	N/A	Noise	60
	Left & right buttons	Press down	60 of each (120 total)
	Both buttons	Simultaneous press	60
	N/A	Noise	60
Total			1,380

Table 1: The data collected during our in-lab sessions.

A laptop was used for recording acoustic data. Likewise, the laptop also received data from a connected camera feed, which served as our visual baseline for inferring user's squeeze strength and behavior.

## Results

We ran a post-hoc analysis to simulate the real-time accuracy assessment with a per-user classifier, which was trained on an individual's own training data samples. We separated each participant's data into nine sets and applied 10-fold cross validation to train the classifier. The mean accuracy for the gamepad, the interactive bunny, and the smart case was: 99.4% ( $SD=0.7\%$ ), 98.2% ( $SD=1.3\%$ ), and 100% ( $SD=0\%$ ) (Figure 9). This demonstrates high robustness for per-user training. Particularly, the smart case is favorably perfect in this case.

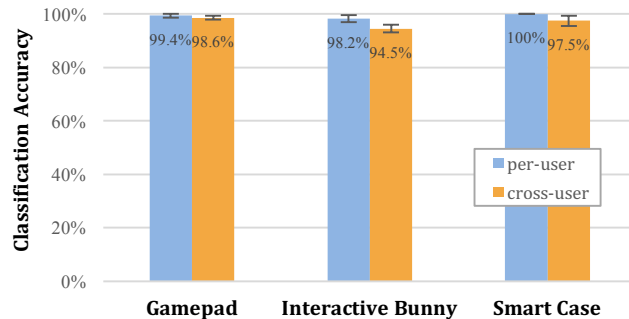


Figure 9. Classification Accuracy of per-user classifier (blue) vs. cross-user classifier (orange) for three applications: gamepad, interactive toy, and smart case.

We also conducted a second post-hoc analysis to examine if our approach worked across users. We estimated the performance by using a general classifier excluding that user's data for training. We trained the classifier using data from eight participants and tested using data from ninth participant with all combinations (*i.e.*, 9-fold cross validation). Figure 11 shows the results: the mean accuracy for the gamepad, the interactive bunny and the smart case were 98.6% ( $SD=0.8\%$ ), 94.5% ( $SD=1.4\%$ ), and 97.5% ( $SD=1.9\%$ ). Overall, cross-user classification accuracy is, as expected, lower than per-user classification; however, accuracy is still well above 90% demonstrating the generalizability of our approach.

The confusion matrices from our cross-user classification experiments shown in Figure 10 help uncover sources of error. For the gamepad, a major source of error was 4.4% of *Other* (*i.e.*, illegal input) events were classified as *Bottom Button Up* events. In the interactive bunny, 16.1% of *Press* input was incorrectly classified as *Poke* input. This is likely because both interactions compress the belly cavity and the resulting air flow through the two corrugated tubes creates a similar signature. Furthermore, another error happened between the category of *Right ear* and *Both Ears*, contributing 33.7% of the misclassified instances. Among the two soft buttons on the smart case, most of the error was caused between *Right Button* squeezing and *Both Buttons* squeezing, which had 66.7% of the misclassifications.

## Supplementary Study: Noise Robustness

To further investigate the robustness of our approach to sound noise in various environments, we tested the gamepad controller in both a quiet office (~51dB) and a noisy coffee shop (~80dB) separately with 5 participants from the previous study. In both situations, we ran 20 trials, and each trial had 27 random inputs (*e.g.*, press down on top button, click center button, *etc.*) on the gamepad's soft buttons. In total, we collected 540 inputs. We then counted the number of correctly detected events to compute the accuracy. In this experiment, the accuracy of correctly detected button squeezing was 98.1% ( $SD=1.0\%$ ) in the quiet place and 96.8% ( $SD=1.5\%$ ) in the noisy environments. While slightly lower in the coffee shop, these results demonstrate our approach's general robustness to noise.

## DISCUSSION

Although our user studies show promising results, some limitations exist. First, as with other acoustic-based sensing techniques, ambient noise has a small but undesirable impact on accuracy. One possible solution is to add sound damping material (*e.g.*, sponge) around the microphone for noise reduction. Additionally, sensing is not possible for very slow presses since airflow is weak and barely detectable by the microphone. Our corrugated tube designs offer capabilities for tracking noticeable changes in air energy at the moment of pressing buttons or exerting discrete force. Thus, our force sensing example can detect the magnitude of discrete presses, but not continuous pressure trajectories.

Further, the act of squeezing exacts physical wear and tear to prototyped objects. We suspect that this could alter the object's acoustic response over time. We did not perform any long-term evaluations, but generally, holes in pipes or cavities will ultimately affect the air pressure flowing across the corrugated channel. Future studies should stress test the system by manually poking holes and monitoring accuracy degradation. We suggest follow-up investigations that examine whether the machine learning model will still work *e.g.*, six weeks after it was trained.

Nonetheless, our approach can be easily extended to support

	Left Ear	0	0.5	0	0	0	0	0	0.5
Left Ear	99	0	0.5	0	0	0	0	0	0.5
Right Ear	1.1	90.6	8.3	0	0	0	0	0	0
Two Ears	4.4	8.3	87.3	0	0	0	0	0	0
Right Hand	0	0	0	100	0	0	0	0	0
Left Hand	2.8	0	0	0	97.2	0	0	0	0
Two Hands	0.6	0	0	1.7	2.2	95.5	0	0	0
Poke	0	0	0	0	0	0	98.6	1.4	0
Press	0	0	0	0	0	0	16.1	83.9	0
Other Noise	0.6	0	0	0	0	1.1	0	0	98.3

(a) Interactive Bunny ( $N=4860$ )

	Top Button Down	0	0	0	0	0	0	0	0
Top Button Up	100	0	0	0	0	0	0	0	0
Right Button Down	0	98.3	0	0	0	1.1	0	0	0.6
Right Button Up	0	0	0	99.4	0	0.6	0	0	0
Bottom Button Down	0	0	0	0	98.9	0	0	0	1.1
Bottom Button Up	0	0	0	0	0	100	0	0	0
Left Button Down	0	0	0	0	0	0	100	0	0
Left Button Up	0	0	0	0	0	0	0	100	0
Central Button Click	0	0	0	0	0	1.7	0	0.6	97.7
Other	1.1	0	0	0	0	4.4	0	0	93.9

(b) Gamepad ( $N=5400$ )

	left	100	0	0	0
right	0.6	95	4.4	0	
both	1.1	2.2	97	0	
other	0.6	1.1	0	98	

(c) Smartphone case ( $N=2160$ )

**Figure 10. Confusion matrix of classification accuracies from our cross-user studies.** Each cell indicates the percentage of squeeze trials assigned to a predicted class (row) for each actual class (column). N=number of total squeeze trials.

any interaction that can generate puffs of air as input. Specifically, we can integrate blowable, hands-free interaction to wearables or fabricated objects by implanting them with corrugated tubes. For instance, by 3D printing a porous air plane and channeling those holes on the surface to the corrugated tubes and the microphone, we are able to interact with the plane by blowing interactions (Figure 11). Here, we eliminate the need for squeezable cavities altogether. Unlike BLUI [22], interaction is not limited to flat surfaces (screens); single channel, linear arrays, and non-planar localization can be achieved with a single microphone. Overall, this extends to any interaction that integrates pulses or streams of air.



**Figure 11. The blowable air plane:** blowing toward the holes on the surface to interact with this 3D-printed plane.

Finally, our corrugated tubes are easy to fabricate and reusable. However, fabricating corrugated tubes using traditional 3D printing techniques requires a specific operating range. Notably, a 3D printer should be able to print tube-like structures with diameters between 1.6-3.2 mm. Our corrugated tubes were printed on clear UV-cured photopolymer (Objet Connex). More recently, we have experimented with common FDM materials (*i.e.*, PLA, ABS) on consumer-grade printers (*e.g.*, MakerBot), which worked but with modifications to the corrugated structures (*e.g.*, we smoothed the corrugations to avoid support materials) to account for lower-resolution prints. While our soft cavities were created with silicon molds, we believe future 3D printers, which can combine multiple filament

materials (*e.g.*, with flexible and standard filament), could create Squeezapulse designs in a single print.

## CONCLUSION

In this paper, we introduced Squeezapulse, a technique to embed soft, low-cost, passive air structures for prototyping and fabrication of interactive objects. The air pulses generated by squeezing the soft cavity embedded in fabricated objects are detected as interactive input through a reusable and uniquely designed corrugated tube. Multiple inputs can be detected by a shared and attachable microphone, without an external sustained sound source or circuitry. We described a machine learning-based acoustic sensing approach for recognizing air pulses, experimented with a set of corrugated tube designs, and demonstrated the feasibility and accuracy of our approach with four example applications and a user study.

## REFERENCES

1. Eric Brockmeyer, Ivan Poupyrev, and Scott Hudson. 2013. PAPILLON: designing curved display surfaces with printed optics. Proceedings of the 26th annual ACM symposium on User interface software and technology - UIST '13: 457–462. <http://doi.org/10.1145/2501988.2502027>
2. W. Burstyn. 1922. Eine neue Pfeife (a new pipe). Tech. Phys 3: 179–180.
3. Luc Geurts, Vero Vanden Abeele, Karen Vanderloock, Jolien Deville, and Jelle Saldien. 2014. Skweezee Studio: Turn your own plush toys into interactive squeezable objects. Proceedings of the 8th International Conference on Tangible, Embedded and Embodied Interaction - TEI'14: 377–380. <http://doi.org/10.1145/2540930.2567896>
4. Luc Geurts. 2013. Skweezees : Soft Objects that Sense their Shape Shifting.
5. Sidhant Gupta, Daniel Morris, Shwetak Patel, and Desney Tan. 2012. SoundWave: Using the Doppler Effect to Sense Gestures. Proceedings of the 2012 ACM annual conference on Human Factors in Computing Systems - CHI '12: 1911–1914. <http://doi.org/10.1145/2207676.2208331>

6. Chris Harrison and SE Scott E Hudson. 2008. Scratch Input: Creating Large, Inexpensive, Unpowered and Mobile Finger Input Surfaces. Proceedings of the 21st Annual ACM Symposium on User Interface Software and Technology: 205–208.  
<http://doi.org/10.1145/1449715.1449747>
7. Chris Harrison, Robert Xiao, and Scott Hudson. 2012. Acoustic barcodes: passive, durable and inexpensive notched identification tags. 1–5.  
<http://doi.org/10.1145/2380116.2380187>
8. Scott E Hudson. 2014. Printing Teddy Bears : A Technique for 3D Printing of Soft Interactive Objects. Proceedings of the SIGCHI Conference on Human Factors in Computing Systems: 459–468.  
<http://doi.org/10.1145/2556288.2557338>
9. Sungjae Hwang, Andrea Bianchi, and Kwang-yun Woon. 2012. MicPen : Pressure-Sensitive Pen Interaction Using Microphone with Standard Touchscreen. 1847–1852.
10. Gota Kakehi, Yuta Sugiura, Anusha Withana, et al. 2011. FuwaFuwa: Detecting Shape Deformation of Soft Objects Using Directional Photoreflectivity Measurement. ACM SIGGRAPH 2011 Emerging Technologies: 5:1–5:1.  
<http://doi.org/10.1145/2048259.2048264>
11. Gierad Laput, Eric Brockmeyer, Scott E. Hudson, and Chris Harrison. 2015. Acousturments: Passive, Acoustically-Driven, Interactive Controls for Handheld Devices. Proc. CHI: 2161–2170.  
<http://doi.org/10.1145/2702123.2702414>
12. Dingzeyu Li and David I W Levin. Acoustic Voxels : Computational Optimization of Modular Acoustic Filters.
13. Chin-yu Chien Rong-hao Liang, Long-fei Lin Liwei, and Chan Bing-yu Chen. FlexiBend : Enabling Interactivity of Multi-Part , Deformable Fabrications Using Single Shape-Sensing Strip. Figure 1: 3–7.
14. Patrizia Marti. 2015. Evaluating the Experience of Use of a Squeezable Interface. SEPTEMBER 2015: 42–49.  
<http://doi.org/10.1145/2808435.2808461>
15. V Marynel, Eric Brockmeyer, and Ruta Desai. 2015. 3D Printing Pneumatic Device Controls with Variable Activation Force Capabilities.
16. Adiyan Mujibiya, Xiang Cao, Desney S Tan, Dan Morris, Shwetak N Patel, and Jun Rekimoto. 2013. The Sound of Touch : On - body Touch and Gesture Sensing Based on Transdermal Ultrasound Propagation. 189–198.  
<http://doi.org/10.1145/2512349.2512821>
17. Roderick Murray-Smith, John Williamson, Stephen Hughes, and Torben Quaade. 2008. Stane: Synthesized Surfaces for Tactile Input. Proceedings of the SIGCHI Conference on Human Factors in Computing Systems: 1299–1302. <http://doi.org/10.1145/1357054.1357257>
18. Ryuma Niiyama, Xu Sun, Lining Yao, Hiroshi Ishii, Daniela Rus, and Sangbae Kim. 2015. Sticky Actuator: Free-Form Planar Actuators for Animated Objects. Proceedings of the Ninth International Conference on Tangible, Embedded, and Embodied Interaction - TEI '14: 77–84. <http://doi.org/10.1145/2677199.2680600>
19. Makoto Ono, Buntarou Shizuki, and Jiro Tanaka. 2013. Touch & activate: adding interactivity to existing objects using active acoustic sensing. Proceedings of the 26th annual ACM symposium on User interface software and technology: 31–40.  
<http://doi.org/10.1145/2501988.2501989>
20. Jifei Ou, Gershon Dublon, Chin-yi Cheng, Felix Heibeck, Karl Willis, and Hiroshi Ishii. 2016. Cilllia - 3D Printed Micro-Pillar Structures for Surface Texture , Actuation and Sensing. c.
21. Joseph A Paradiso, Che King Leo, Nisha Checka, and Kaijen Hsiao. 2002. Passive Acoustic Sensing for Tracking Knocks Atop Large Interactive Displays. Proceedings of the 2002 IEEE International Conference on Sensors 1: 521–527.  
<http://doi.org/10.1109/ICSENS.2002.1037150>
22. Shwetak N Patel and Gregory D Abowd. 2007. Blui. Proceedings of the 20th annual ACM symposium on User interface software and technology - UIST '07: 217. <http://doi.org/10.1145/1294211.1294250>
23. Huaishu Peng, Jennifer Mankoff, Scott E. Hudson, and James McCann. 2015. A Layered Fabric 3D Printer for Soft Interactive Objects. Proceedings of the 33rd Annual ACM Conference on Human Factors in Computing Systems - CHI '15: 1789–1798.  
<http://doi.org/10.1145/2702123.2702327>
24. B. Rajavel and M. G. Prasad. 2013. Acoustics of Corrugated Pipes: A Review. Applied Mechanics Reviews 65, 5: 050000.  
<http://doi.org/10.1115/1.4025302>
25. Matthew Reynolds, Alexandra Mazalek, and Glorianna Davenport. 2007. An acoustic position sensing system for large scale interactive displays. 2007 IEEE Sensors: 1193–1196.  
<http://doi.org/10.1109/ICSENS.2007.4388622>
26. Valkyrie Savage, Colin Chang, and B Hartmann. 2013. Sauron: embedded single-camera sensing of printed physical user interfaces. Proceedings of the 26th annual ACM symposium on User interface software and technology: 447–456.  
<http://doi.org/10.1145/2501988.2501992>
27. Valkyrie Savage, Andrew Head, Björn Hartmann, Dan B. Goldman, Gautham Mysore, and Wilmot Li. 2015. Lamello: Passive Acoustic Sensing for Tangible Input Components. Proceedings of the 33rd Annual ACM

- Conference on Human Factors in Computing Systems - CHI '15: 1277–1280.  
<http://doi.org/10.1145/2702123.2702207>
28. Valkyrie Savage, Ryan Schmidt, Tovi Grossman, George Fitzmaurice, and Björn Hartmann. 2014. A Series of Tubes: Adding Interactivity to 3D Prints Using Internal Pipes. Proceedings of the 27th annual ACM symposium on User interface software and technology - UIST '14: 3–12.  
<http://doi.org/10.1145/2642918.2647374>
29. Valkyrie Savage, Xiaohan Zhang, and Björn Hartmann. 2012. Midas: Fabricating Custom Capacitive Touch Sensors to Prototype Interactive Objects. Proceedings of the 25th annual ACM symposium on User interface software and technology - UIST '12: 579–588.  
<http://doi.org/10.1145/2380116.2380189>
30. Catherine Schmidt-jones. 2011. Standing Waves and Wind Instruments 2 What Makes the Standing Waves in a Tube. *Most*: 1–10.
31. Lei Shi, Idan Zelzer, Catherine Feng, and Shiri Azenkot. 2016. Tickers and Talker: An Accessible Labeling Toolkit for 3D Printed Models. Proceedings of the 2016 CHI Conference on Human Factors in Computing Systems: 4896–4907.  
<http://doi.org/10.1145/2858036.2858507>
32. Ronit Slyper and Jessica Hodgins. 2012. Prototyping Robot Appearance, Movement, and Interactions Using Flexible 3D Printing and Air Pressure Sensors. Proceedings of the 21st IEEE International Symposium on Robot and Human Interactive Communication - ROMAN'12 1: 6–11.  
<http://doi.org/10.1109/ROMAN.2012.6343723>
33. Ronit Slyper, Ivan Poupyrev, and Jessica Hodgins. 2011. Sensing Through Structure: Designing Soft Silicone Sensors. Proceedings of the fifth international conference on Tangible, embedded, and embodied interaction - TEI '11: 213–220.  
<http://doi.org/10.1145/1935701.1935744>
34. Karen Vanderloock, Vero Vanden Abeele, Johan A.K. Suykens, and Luc Geurts. 2013. The skweezee system: enabling the design and the programming of squeeze interactions. Proceedings of the 26th Annual ACM Symposium on User Interface Software and Technology: 521–530.  
<http://doi.org/10.1145/2501988.2502033>
35. Martin Weigel, Tong Lu, Gilles Bailly, Antti Oulasvirta, Carmel Majidi, and Jürgen Steimle. 2015. iSkin: Flexible, Stretchable and Visually Customizable On-Body Touch Sensors for Mobile Computing. Proceedings of the 33rd Annual ACM Conference on Human Factors in Computing Systems - CHI '15: 2991–3000. <http://doi.org/10.1145/2702123.2702391>
36. Karl Willis, Eric Brockmeyer, Scott Hudson, and Ivan Poupyrev. 2012. Printed optics: 3D printing of embedded optical elements for interactive devices. Proceedings of the 25th annual ACM symposium on User interface software and technology - UIST '12: 589–598. <http://doi.org/10.1145/2380116.2380190>
37. Lining Yao, Ryuma Niiyama, Jifei Ou, Sean Follmer, Clark Della Silva, and Hiroshi Ishii. 2013. PneUI: Pneumatically Actuated Soft Composite Material s for Shape Changing Interfaces. Proceedings of the 26th annual ACM symposium on User interface software and technology - UIST '13: 13–22.  
<http://doi.org/10.1145/2501988.2502037>